XII International Conference on Computational Plasticity. Fundamentals and Applications
COMPLAS XII
E. Oñate, D.R.J. Owen, D. Peric and B. Suárez (Eds)

THERMOMECHANICAL STUDY OF NANOVOID CAVITATION IN ALUMINIUM

M.P. ARIZA*, M. PONGA† AND M. ORTIZ†

*Escuela Técnica Superior de Ingeniería, Universidad de Sevilla
Camino de los descubrimientos, s.n. 41092-Sevilla, Spain
E.-mail: mpariza@us.es, http://personal.us.es/mpariza/

† Division of Engineering and Applied Science, California Institute of Technology,
1200 E. California Blvd. Pasadena, 91125 CA, USA.
E-mail: mponga@caltech.edu ortiz@aero.caltech.edu

Key words: Multiscale modeling; Nanovoids; Plasticity; Quasicontinuum method

Abstract. Defects such as vacancies and nanovoids are known to drastically modify the structural state of materials. Void nucleation, growth and coalescence are important micromechanical mechanisms underlying ductile crack growth in metals. In high-purity metals, void nucleation often operates at the nanoscale and is followed by plastic cavitation when the void attains the critical pressure for dislocation emission. This work is concerned with the thermomechanical study of plastic nanovoid cavitation in aluminium (Al) single crystals under triaxial load using the HotQC method. HotQC is a multiscale modeling scheme that seamlessly links continuum and atomistic descriptions at finite temperature. This work provides a detailed characterization of the void growth and cavitation mechanism, including the emitted dislocations, the dislocation reaction paths and attendant macroscopic quantities of interest such as the cavitation stress and temperature evolution as well as a comparison with a previous work carried out at $0K$.

1 INTRODUCTION

The complete mechanism of ductile failure in metals induced by the presence of voids is divided in three main stages, for instance: *void nucleation*, *cavitation* and *coalescence* [1]. This failure mechanism has been documented by many experimental works [2, 3] and references therein. The nucleation of nanovoids at the atomistic scale of the material might occur due to different mechanisms, such as vacancy diffusion in high-purity metallic single crystals under extreme conditions, i.e. plastic deformation, shock wave loading, etc. [4]. Nanovoids can also appear in crystals under extreme loading conditions in order to accommodate the applied deformation or can be due to defects during the manufacturing process of the material, which is observed even in highly pure synthesized nanomaterials

[5]. The following stage in ductile failure is the void growth. In this stage, the nanovoid increases its volume multiple times in order to accommodate the applied stress, starting the plastic deformation and dislocation emission from the surface of the void. Finally, when the size of the void is sufficiently large to interact with other voids the coalescence process is observed. Therefore, the damage in the material is characterized by the emergence of distributed microcracks or voids in a narrow region of the material which may result in the catastrophic failure of the specimen.

Due to the fact that ductile failure of materials is one of the main mechanism of failure in many different engineering devices, we focus our work in the study of nanovoid growth by dislocation emission to understand the onset of plastic cavitation. This problem has been analysed by many works using Molecular Dynamic (MD) simulations [6, 7, 8] to mention but a few. Although MD is particularly well suited for the study of void growth at very high strain rates, this method does not allow to simulate the thermodynamic evolution of the material during the ductile failure. In order to overcome this limitation, in this work we use a novel approach for simulating thermomechanical problems based on the multiscale approach proposed by the Quasicontinuum method (QC). The QC methodology was proposed more than fifteen years ago [9] as a modeling approach for the study of mechanical problems where atomistic resolution is required in a localized subset of the analysis domain. Initially, the QC was applied to the solution of mechanical problems in solids with defects at $0K$. More recently, the method has been extended to encompass coupled non-equilibrium thermomechanical problems [10, 11], enabling the full analysis of continuum/atomistic domains of materials at finite temperature. This extension is called HotQC method and has been applied to different plasticity problems such as nanoindentation [10] and nanovoid growth under triaxial expansion [11, 12]. HotQC method is used in this work as the multiscale approach to study the thermomechanical evolution of the void growth by dislocation emission in aluminum under triaxial loading conditions.

The development of the HotQC method for non-homogeneous temperature distributions relies on three aspects. Firstly, the instantaneous vibrations of the atoms are eliminated through the use of the Jayne's maximum entropy principle [13], performing phase average and constructing a mean field free energy, which is function of the macroscopic variables of the atoms such as position, temperature and frequency. Secondly, a variational thermoelastic formulation proposed by Yang *et al.* [14] is required in order to describe equilibrium and away-from-equilibrium thermodynamics of solids. Third, a coarse-graining of the full thermodynamic problem must allow bridging the continuum and atomistic scales. One of the main advantages of the HotQC method, is that we can set up different time steps between thermodynamic equilibrium solutions, and therefore, we can simulate systems in different thermodynamic states, varying from isothermal (large time steps) to adiabatic (very small time steps).

In this work we focus our study on the evolution of nanovoid growth by dislocation emission in single Al crystals at finite temperature. Our intention is to study the effect of the temperature in the cavitation stress, void growth and dislocation emission. To this

end, we compare our results with those from the previous work of Marian *et al.* [15] where they applied the QC method at $0K$ to study nanovoid cavitation by dislocation emission in aluminum single crystals.

2 SIMULATION DETAILS

The simulation performed in this work was carried out using the following set up. The computational domain Ω_{RV} is a cubic crystal of aluminium of dimensions $144a_0 \times 144a_0 \times 144a_0$ ($a_0 = 4.032\mathring{A}$). We used the EAM-type potentials proposed by Ercolessi *et al.* [16] to simulate Al under triaxial expansion at the strain rate $\dot{\varepsilon} = 10^{10}s^{-1}$. In the center of the crystal a cubic full atomistic zone of dimensions $16a_0 \times 16a_0 \times 16a_0$ is provided. Away from the full representative zone we apply systematically coarsening of the sample Ω_{RV} using a set of representative atoms or nodes. Therefore, a Finite Element (FE) mesh is defined using a Delaunay triangulation over the nodes. In the center of Ω_{RV}, a spherical void of diameter $12.5a_0$ is modeled by removing atoms from the initial full atomistic zone. Firstly, the sample is initially relaxed at an initial temperature $T_0 = 300K$, this is performed by the minimization of the mean field free energy with respect to the nodal positions $\{\mathbf{q}_a\}$ and frequencies $\{\omega_a\}$. For the thermal expansion, the Boundary Conditions (BCs) applied to the sample consists on fixing the normal displacement at nodes on planes $x = 0$, $y = 0$ and $z = 0$. This BC ensures isothermal expansion preventing the distortion of the crystal. After the initial thermal expansion, the computational cell is deformed applying a homogeneous deformation gradient, where the deformation increment is set up as 0.1%. The applied BCs for this part of the simulation start with the removal of the initial applied restrictions. Then, we proceed by imposing a given displacement of the atoms located at the free surfaces of the crystal and finding the equilibrium positions of the remaining ones by minimizing the mean field free energy. In every deformation step, the equilibrium configuration is found using a nonlinear conjugate gradient method [17]. Alternatively, a dynamic relaxation method is used [18] when the computational minimization process during a loading step becomes very slow. In addition, the atomic temperature is allowed to change between steps of deformation and the equilibrium value for each atom is reached by using a nonlinear conjugate gradient which guarantees the maximization of the total energy with respect to the nodal temperatures $\{T_a\}$. Additionally, in order to ensure full atomistic resolution when dislocations are emitted, an automatic remeshing scheme of the FE mesh is performed as a function of the second invariant of the Lagrange strain tensor. Finally, atoms that belong to the dislocation cores are distinguished based on their dimensionless Centro Symmetric Deviation (CSD) parameter [19] computed using the Atomeye program [20]. To ease the comparison of our results with those previously obtained by Marian *et al* [15], in all subsequent dislocation structure plots, atoms are coloured according to the relative magnitude of their CSD parameter with red corresponding to perfect dislocation cores, while atoms belonging to anomalous dislocations are identified by means of a green-yellow color, following their coloring criteria.

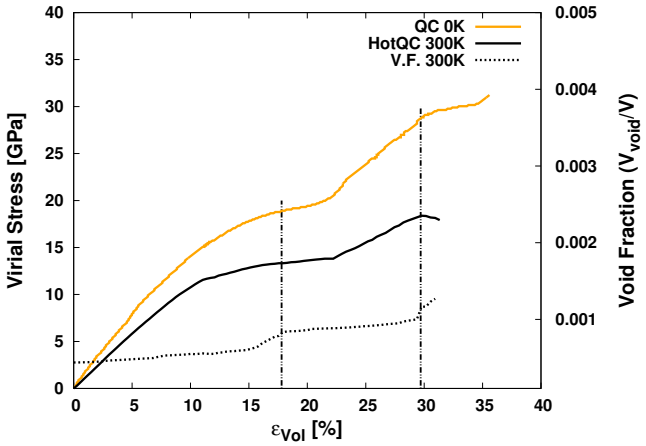

Figure 1: Virial stress *vs* volumetric deformation for Al under triaxial expansion. Results presented in [15]at $0K$ compared with finite temperature results obtained using HotQC (the simulation at finite temperature is carried out at $T_0 = 300K$ and $\dot{\epsilon} = 10^{10}s^{-1}$). Also, the void fraction (V_{void}/V) is plotted for the finite temperature simulation.

3 RESULTS

In this section we proceed to describe the evolution of the virial stress *vs* volumetric deformation, the dislocation structures and kinetics at the early stages of the void growth, the subsequent void shape changes and the atomic temperature field evolution in Al single crystal obtained using the HotQC method.

3.1 Stress *vs* strain and void fraction curves

Figure 1 shows the evolution of the virial stress *vs* strain for the simulation performed at $0K$ by Marian *et al.* [15] as well as the curve for finite temperature obtained using the HotQC method. Both simulations were carried out using the interatomic potential proposed by Ercolessi *et al.* [16]. The void fraction evolution (V_{void}/V) for $T_0 = 300K$ is also shown in Figure 1. We observe a reduction of the cavitation stress at finite temperature of about 30% which is expected due to the evolution of the elastic modulus with the temperature. Although the evolution of both curves is quantitatively different, the behaviour of the material is qualitatively similar in both simulations. The evolution of the virial stress might clearly be divided in three different stages easily identified by means of the void fraction curve. These three main stages are summarized as: i) a first stage up to the first cavitation point at $\epsilon_{Vol} = 17.2\%$ for the $0K$ simulation and $\epsilon_{Vol} = 16.9\%$ for the simulation at finite temperature, characterized by elastic expansion of the void without dislocation emission, ii) following this linear stage, a second plastic stage up to the second cavitation point at $\epsilon_{Vol} = 30.8\%$ for $0K$ and $\epsilon_{Vol} = 29.9\%$ for $T_0 = 300K$, characterized by the emission of dislocations from the void surface and plastic void growth, iii) finally,

a third stage of hardening is observed in the simulation performed at $0K$ whereas for the finite temperature case, we observe a loss of stiffness in the crystal up to its failure.

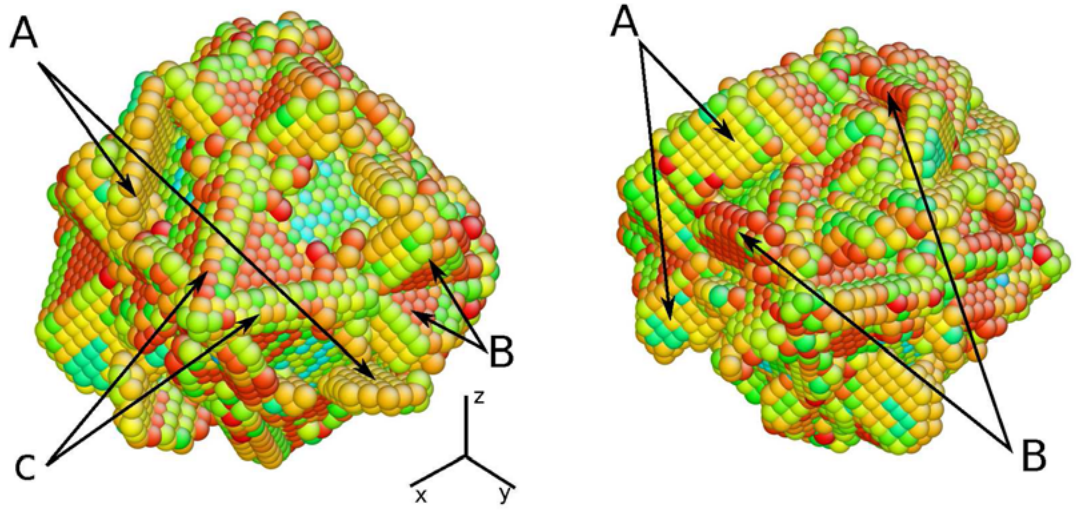

(a) (b)

Figure 2: Dislocation structures around the void for the first cavitation point observed at finite temperature. Front (Figure 2a) and back (Figure 2b) view of dislocation structure. Anomalous dislocations $b = \frac{1}{2}\langle 110\rangle$ on $\{001\}$ planes are labelled with letter A, perfect dislocations $b = \frac{1}{2}\langle 110\rangle$ on $\{111\}$ planes are labelled with letter B and Lomer-Cottrell dislocations are labelled with letter C.

3.2 Dislocation emission

During the first stage of the loading process we have observed a linear deformation of the void, the crystal does not bear any plastic deformation nor dislocation emission. When the stress reaches the critical value for dislocation emission, the cavitation process starts and the dislocations are emitted from the void surface. We proceed to describe and compare the dislocation structures predicted by the QC method [15] and our results at finite temperature. Figure 2 of reference [15] shows the dislocation structure observed just after the first cavitation point, which is composed of a set of tetrahedral dislocation junctions symmetrically distributed on all six $\langle 100\rangle$ vertex of the void. A detailed analysis of the dislocation structures performed by the authors reveals sets of four tetrahedra converging at a single point. The tetrahedra is composed of $\{111\}$ stacking fault surfaces bounded, alternatively, by stair-rod type sessile dislocations, with Burgers vector $b = 1/6\langle 110\rangle$, and perfect dislocations $b = 1/2\langle 110\rangle$.

Figure 2 shows the dislocation structure obtained for the first cavitation point at $T_0 = 300K$. Figures 2a and 2b correspond to the front view and the back view of

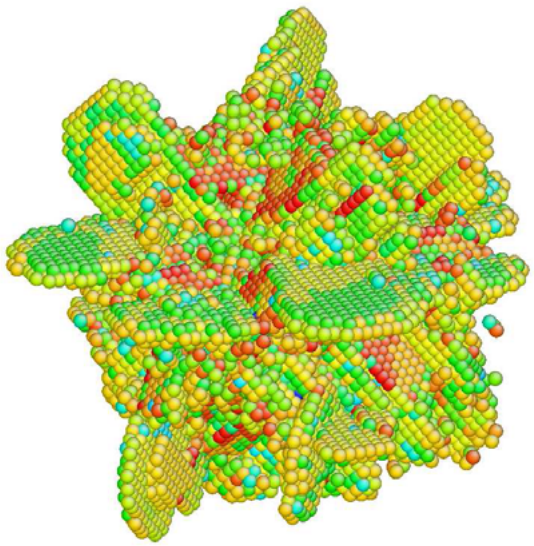

Figure 3: View of the dislocations structure surrounding the void at $\epsilon_{Vol} = 32.0\%$ at finite temperature. We can observe the anomalous type dislocations $b = \langle 110 \rangle$ on $\{001\}$ planes and the perfect type dislocations $b = \langle 110 \rangle$ on $\{111\}$ planes.

the dislocation structures form after the first cavitation point at $T_0 = 300K$. As we can see, a different structure is obtained by our finite temperature simulation, this dislocation configuration is less rigid than the one in reference [15]. However, the type of dislocations emitted from the void surface together with the active slip systems are the same for both simulations. For the finite temperature case, we observe the emission of dislocations with $b = 1/2\langle 110 \rangle$ on planes $\{001\}$ (labelled with letter A) which have also been observed by Marian *et al*, perfect dislocations $b = 1/2\langle 110 \rangle$ on $\{111\}$ planes (labelled with letter B) and Lomer-Cottrell dislocations at $\{001\}$ planes (labelled with letter C). Due to the fact that dislocations of type-A are not common in FCC metals, they called them *anomalous* dislocations. Therefore, we can conclude that the potential proposed by Ercolessi *et al.* predicts the emission of anomalous dislocations with $b = 1/2\langle 110 \rangle$ on planes $\{001\}$ independently of considering the thermomechanical coupling mechanism. In fact, this type of dislocation is the most commonly observed during the process of void growth. This is due to the geometry of the distribution of dislocations, where the anomalous dislocations block the growth of the perfect ones ($b = 1/2\langle 110 \rangle$) when the latter ones reach the $\{001\}$ plane. Indeed, when one perfect dislocation $b = 1/2\langle 110 \rangle$ is emitted, it travels along the crystal on planes $\{111\}$. However, once it reaches the anomalous dislocation at the intersection of the planes $\{111\}$ and $\{001\}$. Then, the $b = 1/2\langle 110 \rangle$ dislocation on $\{111\}$ plane gets blocked due to presence of anomalous dislocations. This mechanism blocks the emission and the interactions between different dislocations in different slips systems and

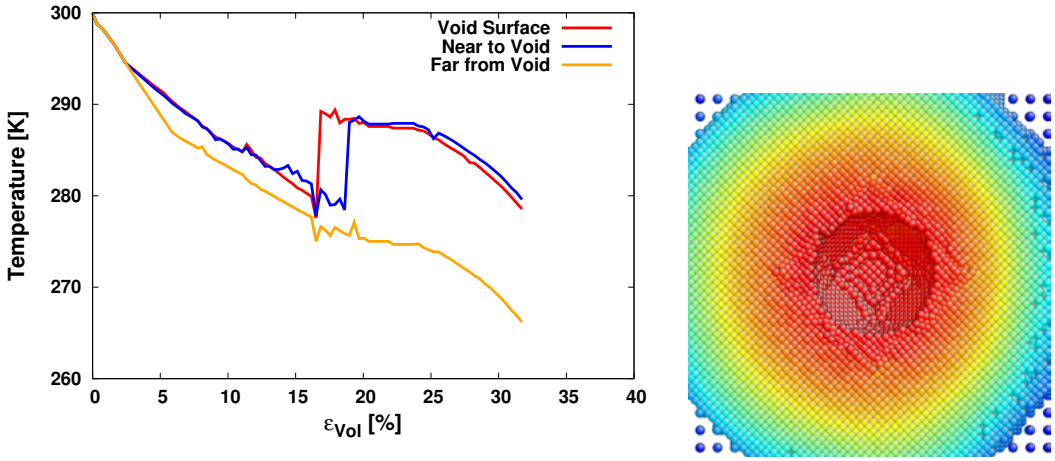

(a) (b)

Figure 4: Temperature evolution and temperature field for Al. Figure 4a shows the evolution of the temperature with the deformation. Figure 4b shows the temperature field along $z = 0$ at $\epsilon_{Vol} = 20\%$.

as result there is no emission of prismatic dislocations loops, which is commonly observed in the evolution of void growth. After reaching the first cavitation point, the anomalous dislocations continue moving away from the void surface. Finally, Figure 3 shows the dislocations structure for $\epsilon_{Vol} = 32.0\%$, just before the crystal collapses.

3.3 Temperature evolution

Figure 4 shows the time-evolution of the temperature observed at three different points within the crystal: one point on the surface of the void, a second point near to the void surface and a third point far from the void surface. Before reaching the critical strain for cavitation, the crystal cools down due to the thermoelastic effect of the material as expected for large strain rates. This variation in the temperature is clearly linear in accordance with the linear deformation of the crystal. However, when the deformation field attains the critical value for the cavitation of the void, the temperature along the void surface experiences an abrupt increment causing a fast heating localized in this zone. Figure 4b represents the atomic temperature filed in the vicinity of the void at $\epsilon_{Vol} = 20\%$. It is easily seen that the temperature field is clearly inhomogeneous, reaching its highest value along the void surface. Additionally, we can observe that when $\epsilon_{Vol} = 20.0\%$ the temperature of the atom labelled as *near to the void* increases its value due to the presence of dislocations at this position. Moreover, during the last steps of deformation, the evolution of the temperature shows a slowdown. This behaviour in the time evolution of the temperature indicates a loss in the global stiffness of the crystal.

3.4 Void growth

The evolution through the cavitation process of the void fraction *vs* volumetric deformation has been presented in Figure 1. We might clearly differentiate three stages in the void fraction evolution. First, a linear regimen up to $\epsilon_{Vol} = 16.7\%$ in which the change in the void volume is proportional to the deformation. This stage is associated with the elastic deformation of the crystal and dislocations are not observed before this point. Then, as deformation increases, atoms at the void surface need to move in order to minimize the energy stored in the crystal due to the applied deformation. This point corresponds with the first cavitation of the void, which might be clearly identified by the sudden increase of its volume. Furthermore, as the deformation increases, the void fraction passes through a linear stage before attaining the second cavitation point, which is reached at approximately $\epsilon_{Vol} = 27.5\%$. At this point, the evolution of the void fraction indicates a sharp increase in the void volume and correspondingly a decrease in the stiffness of the crystal is observed. The further stage of deformation shows a drop of the virial stress *vs* strain curve followed by the global failure of the crystal after some steps of deformation. Additionally, Figure 5 shows several snapshots of the void at different levels of deformation. We observe that prior to cavitation the void maintains its perfect spherical shape (Figures 5(a) and 5(b)). Then, after reaching the first cavitation point (Figure 5(c)) we observe that the void grows primarily in planes $\{111\}$. Finally, snapshots corresponding to the last stages of deformation (Figures 5(d) to 5(f)) show that the void shape becomes more spherical.

4 CONCLUSIONS

We have applied the HotQC method to the study of the thermomechanical evolution of void growth in aluminium single crystals under triaxial expansion and compared our results with the previous work of Marian *et al.* [15]. We have ascertained that the critical stress for dislocation emission is reduced at finite temperature about a 30% in comparison with $0K$ simulations. This result is expected due to the variation of the elastic modulus in materials with temperature. We also observed that upon the attainment of a critical or cavitation strain of the order of $\epsilon_{vol} = 17.0\%$, dislocations are abruptly and profusely emitted from the void and the rate of growth of the void increases precipitously. The simulation carried out in this work shows the emission of different dislocations: anomalous, perfect and Lomer-Cottrell dislocations. Although there is a difference in the dislocations structure obtained at $0K$ and $300K$, the observed type of dislocations and active slip systems for both simulations are the same. In addition, we might conclude that the potential proposed by Ercolessi *et al.* [16] predicts the emission of anomalous dislocations which are not commonly observed in FCC crystals. We have also studied the temperature evolution throughout the simulation at different positions within the sample. Remarkably, prior to cavitation, the crystal cools down due to the thermoelastic effect. By contrast, following cavitation dislocation emission causes rapid local heating in the vicinity of the

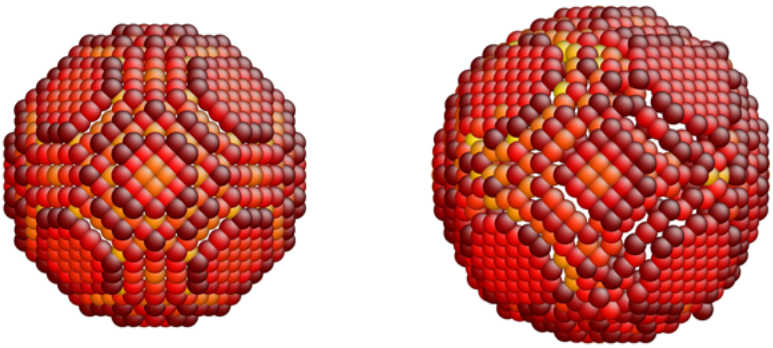

(a) Initial void.

(b) Before cavitation at ϵ_{Vol}= 12.4%.

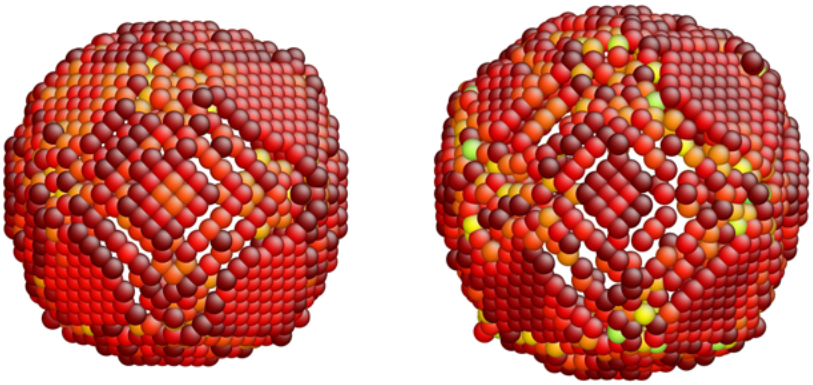

(c) After cavitation $\epsilon_{Vol} = 17.0\%$.

(d) Transition regime $\epsilon_{Vol} = 17.9\%$.

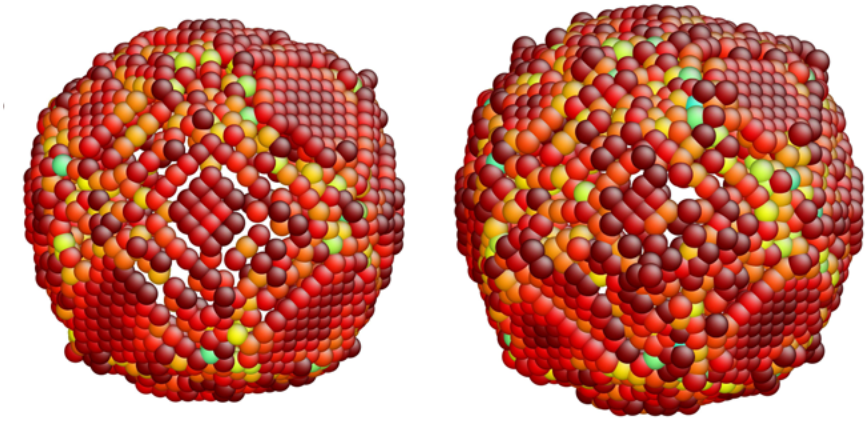

(e) Void at $\epsilon_{Vol} = 21.5\%$.

(f) Void at $\epsilon_{Vol} = 32.9\%$.

Figure 5: Void evolution for [16] potential under triaxial load using the HotQC method. The simulations was carried out at $T_0 = 300K$ and $\dot{\epsilon} = 10^{10}s^{-1}$. All figures are in the same scale.

void, which in turn sets up a temperature gradient and results in the conduction of heat away from the void surface. Our results indicate that a heat flux appears from the void surface and is due to the plastic work generated by the high level of deformation in the surrounding area of the void. Therefore, it bears to emphasize that the study of void cavitation by dislocation emission at finite temperature might be analysed using the coupled thermomechanical framework proposed by the HotQC method.

5 Acknowledgements

We gratefully acknowledge the support of the Ministerio de Ciencia e Innovación of Spain (DPI2009-14305-C02-01) and the support of the Consejería de Innovación of Junta de Andalucía (P09-TEP-4493). Support for this study was also provided by the Department of Energy National Nuclear Security Administration under Award Number DE-FC52-08NA28613 through Caltech's ASC/PSAAP Center for the Predictive Modeling and Simulation of High Energy Density Dynamic Response of Materials.

REFERENCES

[1] V. Tvergaard, "Material failure by void growth to coalescence," vol. 27, pp. 83 – 151, 1989.

[2] R. Bauer and H. Wilsdorf, "Void initiation in ductile fracture," *Scripta Metallurgica*, vol. 7, no. 11, pp. 1213 – 1220, 1973.

[3] A. L. Stevens, L. Davison, and W. E. Warren, "Spall fracture in aluminum monocrystals: a dislocation-dynamics approach," *Journal of Applied Physics*, vol. 43, no. 12, pp. 4922–4927, 1972.

[4] C. Reina, J. Marian, and M. Ortiz, "Nanovoid nucleation by vacancy aggregation and vacancy-cluster coarsening in high-purity metallic single crystals," *Phys. Rev. B*, vol. 84, p. 104117, Sep 2011.

[5] W. Liu, E. Karpov, and H. Park, *Nano Mechanics and Materials: Theory, Multiscale Methods and Applications*. Wileys, 2006.

[6] E. Seppälä, J. Belak, and R. Rudd, "Effect of stress triaxiality on void growth in dynamic fracture of metals: A molecular dynamics study," *Physical Review B*, vol. 69, no. 13, p. 134101, 2004.

[7] E. Bringa, S. Traiviratana, and M. A. Meyers, "Void initiation in fcc metals: Effect of loading orientation and nanocrystalline effects," *Acta Materialia*, vol. 58, no. 13, pp. 4458–4477, 2010.

[8] T. Tsuru and Y. Shibutani, "Initial yield process around a spherical inclusion in single-crystalline aluminium," *Journal of Physics D: Applied Physics*, vol. 40, no. 7, p. 2183, 2007.

[9] E. B. Tadmor, M. Ortiz, and R. Phillips, "Quasicontinuum analysis of defects in solids," *Philosophical Magazine*, vol. 73, pp. 1529–1563, 1996.

[10] Y. Kulkarni, J. Knap, and M. Ortiz, "A variational approach to coarse graining of equilibrium and non-equilibrium atomistic description at finite temperature," *Journal of the Mechanics and Physics of Solids*, vol. 56, pp. 1417–1449, 2008.

[11] M. P. Ariza, I. Romero, M. Ponga, and M. Ortiz, "Hotqc simulation of nanovoid growth under tension in copper," *International Journal of Fracture*, vol. 174, pp. 75–85, 2012.

[12] M. P. Ariza, M. Ponga, I. Romero, and M. Ortiz, "Finite-temperature nanovoid deformation in copper under tension," in *Computational Plasticity XI: Fundamentals and Applications* (Onate, E and Owen, DRJ and Peric, D and Suarez, B, ed.), pp. 1506–1515, 2011.

[13] E. Jaynes, "Information theory and statistical mechanics," *Physical Review*, vol. 106, pp. 620–630, 1957.

[14] Q. Yang, L. Stainier, and M. Ortiz, "A variational formulation of the coupled thermo-mechanical boundary-value problem for general dissipative solids," *Journal of the Mechanics and Physics of Solids*, vol. 54, pp. 401–424, 2006.

[15] J. Marian, J. Knap, and M. Ortiz, "Nanovoid cavitation by dislocation emission in aluminum," *Physical Review Letters*, vol. 93, no. 16, 2004.

[16] F. Ercolessi and J. B. Adams, "Interatomic potentials from first-principles calculations: The force-matching method," *EPL (Europhysics Letters)*, vol. 26, no. 8, p. 583, 1994.

[17] W. T. Vetterling, W. H. Press, B. P. Flannery, and S. A. Teukolsky, *Numerical Recipes Example Book C++*. Cambridge University Press, 2002.

[18] D. R. Oakley and N. F. Knight, "Adaptive dynamic relaxation algorithm for non-linear hyperelastic structures part i. formulation," *Computer Methods in Applied Mechanics and Engineering*, vol. 126, no. 1-2, pp. 67 – 89, 1995.

[19] C. L. Kelchner, S. J. Plimpton, and J. C. Hamilton, "Dislocation nucleation and defect structure during surface nanoindentation," *Physical Review B*, vol. 58, pp. 11085–11088, 1998.

[20] J. Li, "Atomeye: an efficient atomistic configuration viewer," *Modelling and Simulation in Materials Science and Engineering*, vol. 11, no. 2, p. 173, 2003.